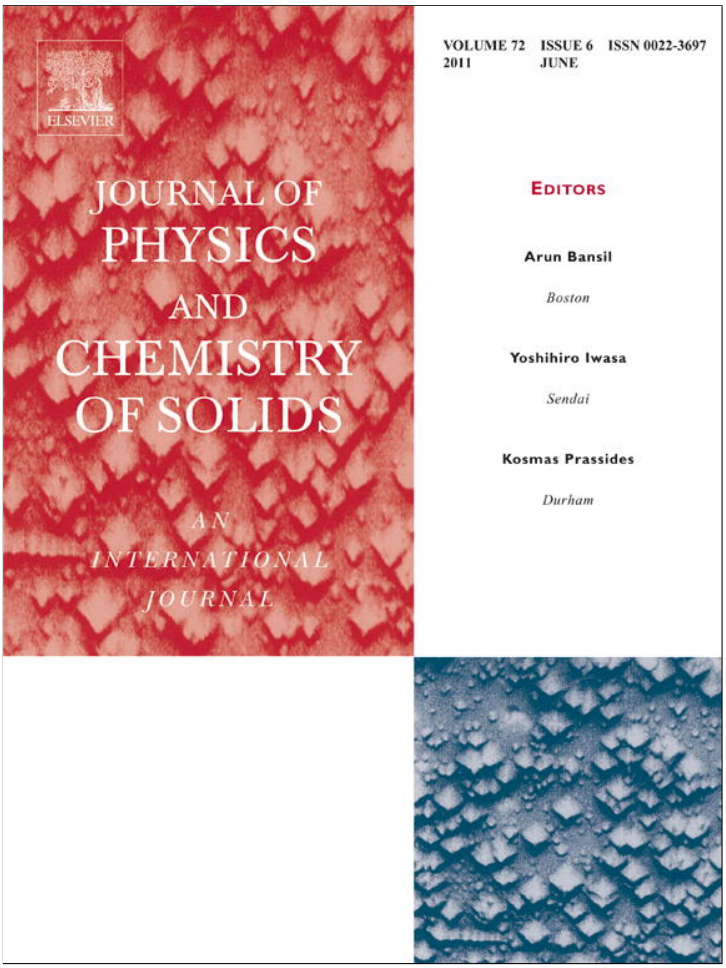

Journal of Physics and Chemistry of Solids 72 (2011) 620–625

Contents lists available at ScienceDirect

Journal of Physics and Chemistry of Solids

journal homepage: www.elsevier.com/locate/jpcs

Thermal stability and reaction properties of passivated Al/CuO nano-thermite

Jeff Wang [a], Anming Hu [a], John Persic [b], John Z. Wen [a,*], Y. Norman Zhou [a]

[a] Department of Mechanical and Mechatronics Engineering, University of Waterloo, 200 University Ave West, Waterloo, ON N2L 3G1, Canada
[b] Microbonds Inc., 151 Amber St, Unit 12 Markham ON L3R 3B3 Canada

ARTICLE INFO

Article history:
Received 22 September 2010
Received in revised form
21 December 2010
Accepted 11 February 2011
Available online 19 February 2011

Keywords:
A. Nanostructures
C. Differential scanning calorimetry
D. Thermodynamic properties

ABSTRACT

Thermal stability and reaction properties of Al–CuO system, a mixture of 50–200 nm aluminum nanoparticles passivated by nitrocellulose and 12 nm copper (II) oxide, were investigated with microstructure characterization, differential thermal analysis (DTA), and thermogravimetric analysis (TGA). Transmission electron microscopy observation confirmed that the passivation coating successfully hinders the oxidization. TGA revealed that the passivation shell does not influence the ignition temperature of the thermite reaction. Reaction chemistry of the nano-thermite was elucidated by heating the composite both in inert ambient and vacuum. It was found that the thermite reaction composes of three continuing steps: At 570 °C, Al is oxidized into Al_2O_3 by reacting with CuO, which forms Cu_2O and produces a significant amount of heat. Subsequently two endothermic reactions occur. Starting at 800 °C, alumina reacts with Cu_2O and forms $CuAlO_2$. Above this temperature $CuAlO_2$ will decompose and eventually produce alumina, Cu, and O_2 at 1000 °C. Since the nano-thermite reaction pathway differs greatly from bulk thermite reactions, these results are important to develop a nano-thermite platform that can be used for a novel low cost, low temperature, and copper based microjoining and advance IC packaging.

1. Introduction

Energetic materials have shown their attractive applications in military, mining, and demolition, thanks to excessive chemical energy released with the ultra-fast reaction rates and by relatively easier ignition methods. Aluminum, as a major component of inorganic energetic composites, has been most commonly investigated for formulating propellants, explosives, and thermites. This is mainly due to its abundance and the relative high energy generation from combustion (the heat of formation of Al_2O_3 is -1675.7 kJ/mol, which is equivalent to -31 kJ per gram of aluminum) [1]. In recent years, researchers have started to use nano-scale reactants to create super-thermites, also known as metastable intermolecular composites (MICs) [2,3]. The classical MIC was obtained by mixing nanoparticles of metallic oxides (e.g., CuO and Fe_2O_3) with a reducing metal such as aluminum. The MIC takes advantage of the unique properties of nano-scale particles, which in general offer the large specific area and lower melting temperature. Since the larger specific area facilitates the faster reaction rate and the depressed melting point, resulting in a lower ignition temperature [4], the MIC has been of great interest in the micro-energetic field where the amount of the reactants is restricted. The MIC has been investigated for developing microthrust, microinitiation, gas actuation, heat supply, and welding [5]. Although these previous studies [6–8] dealt with the MIC composed of aluminum nanoparticles/thin films, a fundamental study on the aluminothermite reaction is still needed. This is particularly due to the sophisticated reaction mechanisms resulting from the size-dependent surface interactions, different mixing mechanisms, and uncertain bulk properties of MIC. On the other hand, due to the active reactivity of aluminum nanoparticles (Al NPs) in air, a thin aluminum oxide passivation layer with a thickness of a few nanometers can quickly form on particles' surface. This characteristic is troublesome for two reasons. First, the content of pure aluminum in the nanoparticle is significantly reduced (e.g., for a 25 nm nanoparticle, a 3 nm oxide shell accounts for $>60\%$ of the volume of the Al NP). Second, the aluminum oxide shell can act as an encapsulation for the core aluminum and thus endures a compressive pressure that hinders the reactivity of the Al NPs [4]. Both affect the thermite reation in a negative way. Recently Chowdhury et al. [9] investigated the ignition mechanism of nano-scale Al/CuO thermites by studying the solid–solid reactions between Al NPs, which had an average diameter of 50 nm and were passivated with an oxide shell with varying thickness and CuO nanoparticles (<100 nm in size). The thermite reactions were studied with a fast heating rate

* Corresponding author. Tel.: +1 519 888 4567; fax: +1 519 885 5862.
E-mail address: jzwen@uwaterloo.ca (J.Z. Wen).

0022-3697/$ - see front matter © 2011 Elsevier Ltd. All rights reserved.
doi:10.1016/j.jpcs.2011.02.006

($\sim 10^5$ K/s). It was found that the ignition temperature was well above the melting point of aluminum (about 1250 K) and an ignition delay was consistent with a diffusion limited reaction rate.

In addition to studying the Al NPs passivated with the aluminum oxide shell, several methods were developed to prevent aluminum oxidation by coating Al NPs with other chemicals. For example, the perfluorocarbon coating of Al NPs was studied by Jouet et al. [10] while the carbon coating and Pd/Ni coating were investigated by Park et al. [11] and Foley et al. [12], respectively. Recently Dubois et al. [13] detailed the coating process of the aluminum and boron nanoparticles with polyolefin and polyurethane. An in situ polymerization process was developed in order to achieve a uniform protective coating of nanoparticles. The effects of the resulting coatings were investigated by characterizing the morphology and the aging behavior of the coated nanoparticles. Two specific aging situations were studied, i.e., in a NaOH solution and under humid conditions. Even though these coated Al NPs have been successfully proved for effectively enhancing the stability of Al NPs, the reaction characteristics of the coated Al NPs as nano-thermite are still not well understood. More specifically, while the coating layer on the Al NP prevents further oxidation, as demonstrated in previous studies, very few studies have focused on the reaction mechanism of the nano-thermite with coated Al NPs as the fuel. In this paper, the Al nanoparticles were coated in a non-aqueous solution by nitrocellulose using a palladium based catalyst. The thermal stability of coated Al NPs was studied by varying the system temperature in the inert and vacuum environment. Note that this study of the thermal stability was different from the previous aging study [13], which was conducted at the room temperature. Moreover, the following aluminothermic reaction between Al NPs and CuO nanoparticles

$$2Al + 3CuO \rightarrow Al_2O_3 + 3Cu \quad (1)$$

was examined in this work specifically for copper-to-copper micro-joining and IC packaging applications.

The research objectives of this study include: first, to demonstrate the reaction feasibility of Al NPs passivated by nitrocellulose; second, to study the ignition of thermite reactions at relatively lower temperatures; thirdly, to elucidate underlying reactions that are important to develop a controlled Al NP based nano-thermite. The microstructures of coated Al NPs and CuO nanoparticles were investigated under transmission electron microscopy (TEM) and scanning electron microscopy (SEM) while the stability and reaction kinetics were studied using thermogravimetric analysis (TGA) and differential thermal analysis (DTA). The chemical compositions were examined using energy-dispersive X-ray spectroscopy (EDX) and powder X-ray diffraction (XRD).

2. Experimental methods

2.1. Preparation and microstructure characterization of nano-thermite mixture

Laser ablated aluminum nanoparticles are very unstable and pyrophoric. Aluminum nanoparticles (Al NP) were passivated with nitrocellulose to resist oxidation [14]. CuO nanoparticles (CuO NPs) with an average size of 12 nm were purchased from Sigma Aldrich and examined using SEM. The mixing between Al NPs and CuO NPs was conducted mechanically. First, the two powders were mixed and crushed finely by a glass rod on a glass plate by hand. Then the powder was further ground and mixed in an alumina mortar. Three mass ratios of Al NPs to CuO NPs were prepared, which were 1:1, 2:1, and 3:1, as shown in Table 1. For the ignition studies, the nano-thermite powder was pressed into pellets to facilitate better mass transport. The nano-thermite was then loaded into a pressing dye with a height of 10 mm and a diameter of 3.2 mm. Roughly 0.020 g of nano-thermite powder was used to fill into the cavity of the dye. The dye was pressed with about 50 MPa of pressure. The dimension of the pellet was consistently 3.2 mm in diameter and 1.43 mm in height. The density of the pellet was 1.8 g/cm^3 on average. The microstructures of the coated Al NPs are characterized by TEM (JOEL2010F). The elemental analysis of the coated Al NPs was done by EDX integrated in the TEM module.

Table 1
Fuel and oxidizer ratio used in thermite reaction experiments.

Al NP:CuO (Mass)	Actual Al:CuO (Mole)	Equivalence ratio ϕ
3:1	3.5:1	1.8
2:1	2.4:1	1.2
1:1	1.2:1	0.6

2.2. Thermal stability and thermite reaction

The stability of the passivation shell was tested and characterized by TGA. The measurements were performed on a TA Instruments Q500 TGA, which operated with two temperature ranges. One measurement used an air purge of 50 ml/min for 25–500 °C. The other used a 50 ml/min N_2 ambient purge for 25–800 °C. The heating rate was set to 10 °C/min. For these measurements, the Al NPs were contained in an alumina pan rather than the conventional platinum pan. This eliminated the possible reactions between alumina and platinum. The elemental analysis from the TGA treated Al NP samples was done by XRD on a Bruker AXS-D8-Advance powder diffractometer operated at 45 kV and 40 mA using the Cu Kα radiation ($\lambda = 1.5418$ Å).

An initial study for the ignition of nano-thermite pellet was done for feasibility purposes. The 3:1, 2:1, and 1:1 ratio nano-thermite pellets were placed on an alumina thermal boat and then heated from room temperature to 800 °C at 10 °C/min in a three-zone tubular furnace (Mellen Company TV-series). Later on, to study the effects of the fuel to oxidizer equivalence ratio and temperature on the reaction kinetics, the nano-thermite pellets were sintered in vacuum in order to eliminate the possible oxygen source from air. For this equivalence ratio study, the 3:1, 2:1, and 1:1 ratio nano-thermites pellets were placed on an alumina thermal boat and heated from room temperature to 1000 °C at 10 °C/min at 0.001 Pa in a high temperature vacuum tube furnace (Barnstead Thermolyne 59300). For the temperature study, the nano-thermite pellets were first placed inside an alumina tube that was 6 cm in length and 5 mm in diameter. The sample was then sealed in a silica tube at 0.1 Pa. The vacuum silica tube was then heated at temperatures of 700, 800, and 900 °C at 10 °C/min in a 3 zone tubular furnace (Mellen Company TV-series). For all furnace tests, the peak temperatures were held for 20 min.

Eq. (2) shows the calculation of the fuel/oxidizer equivalence ratio, ϕ, for different samples. For this study, the core aluminum in the Al NPs is the fuel and the CuO NP is the oxidizer. The mass of the coating nitrocellulose layer, which is roughly 50% of the mass of the Al NP (as shown later by the TGA), was taken away from the calculation. Please note that the value of the 3:1 Al/CuO mass ratio gives $\phi = 1.8$, which is in the range of equivalence ratios studied by Shende et al. [7] with the Al-NP/CuO-nanorod thermite. The maximum combustion speed of nano-thermites in that study was found when $\phi = 1.2$ to 1.8.

$$Equivalnce\ ratio, \phi = \frac{(fuel/oxidizer)_{mass\ of\ actualmix}}{(fuel/oxidizer)_{mass\ based\ rxn\ stoichiometry}} \quad (2)$$

The elemental analysis from the furnace sintered samples was done by XRD using the same equipment mentioned earlier. Temperature dependent structural transformation and the heat release from the nano-thermite reaction were measured using DTA in a NETZSCH Simultaneous Thermal analyzer STA 409 PC. The measurements were done from 0 to 650 °C and from 0 to 1100 °C at a heating rate of 5 °C/min with argon gas purge rate of 80 ml/min. The DTA measurement is calibrated with a sapphire (α-Al_2O_3) blank sample.

3. Results and discussion

3.1. Thermal stability study of passivated Al NPs

Fig. 1(a) shows TEM images of passivated Al NPs with nitrocellulose, which have been exposed to air for 14 days after their synthesis. The size of the coated Al NPs ranges from 50 to 280 nm. A thin coating was observed clearly on all nanoparticles. The coated Al NPs appear to be slightly agglomerated. Fig. 1(b) shows a close-up image taken close to the edge of a coated Al NP. From the top right region C of this image, the single crystalline structure of aluminum is shown clearly. In the middle of the image, there is a black belt (region D, the coating nitrocellulose) between the crystalline and the white TEM grid. The thickness of this coating is about 6 nm. The compositions of different structures in Fig. 1(b) were characterized by the integrated EDX of the TEM, as shown in Fig. 1(c) and (d). The copper signals from the EDX are from the TEM grid and carbon signals from the nitrocellulose. It shows from the region C in Fig. 1(b), which located in the crystalline aluminum zone, that there is a strong presence of aluminum and little other elements could be found. In comparison, Fig. 1(d) shows the EDX pattern taken from the coating nitrocellulose region D. In addition to aluminum, much more carbon and oxygen were observed. Note that, since the EDX signals are a collection of dispersed X-ray spectra over a tear-drop-shape volume below the electron beam, the elemental analysis has a limit to characterize the small region such as the core-shell interface (about 1–2 nm as shown). The composition of the passivated Al NPs is examined more accurately with XRD and will be discussed in the next section.

The TEM images in Fig. 1 clearly demonstrate that the passivation technique was able to add a nano-layer on each particle so that the Al NPs were not highly aggregated or encased in the polymeric block. A low degree of aggregation will allow effective and homogenous mixing of the nano-scale reactants, which improves the mass transport characteristics of the thermite reaction. It is interesting to observe that for these nitrocellulose-coated nanoparticles, a significant amount of active Al content exist after 14 days of their synthesis. This aging behavior is slightly different from the reported polyethylene and polypropylene coated nanoparticles (with the aging periods of 20 to 120 h in humid and at the room temperature) [13]. The discrepancy may result from the different storage conditions and the procedure of coating processes.

Fig. 2 shows the TGA measurement of Al NPs in the inert N_2 and air ambient for the temperature range between 40 and 800 °C. When the temperature increases, the weight of Al NPs decreases by about 50% due to the decomposition and subsequent desorption of the coating material. A two-stage decomposition (at 208 and 322 °C) process was revealed by the derivation of the weight change. This resulted from the degradation and evaporation of nitrocellulose. At 225 °C, the TGA curves in N_2 and air start to deviate. Greater weight loss was found in air due to the greater degradation rate of nitrocellulose in air. The total mass loss from the decomposed coating is about 47% (in N_2) and 49% (in air).

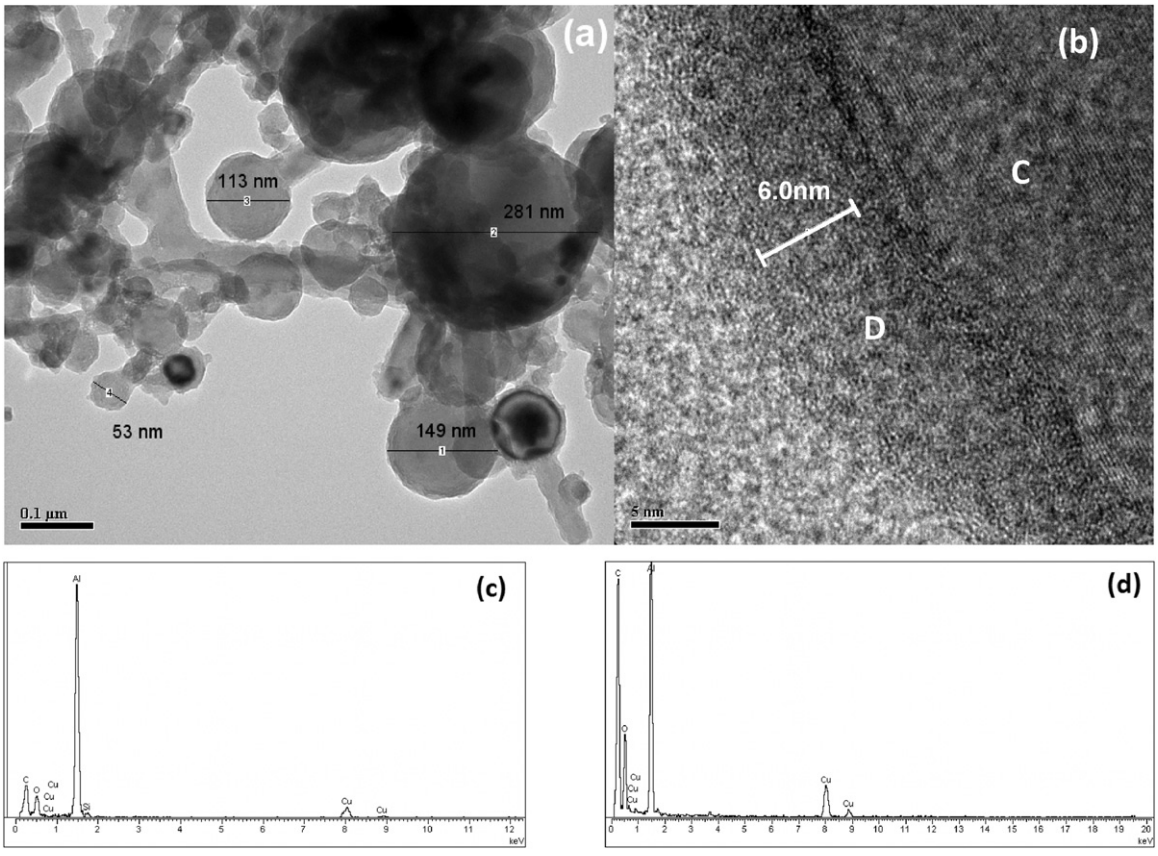

Fig. 1. Low- (a) and high- (b) magnification Transmission Electron Microscope images of passivated aluminum nanoparticles (Al NPs) with a 6 nm nitrocellulose layer. (c) Energy-dispersive X-ray (EDX) spectrum at the region C. (d) EDX spectrum at the region D. EDX was taken at −0.846 keV.

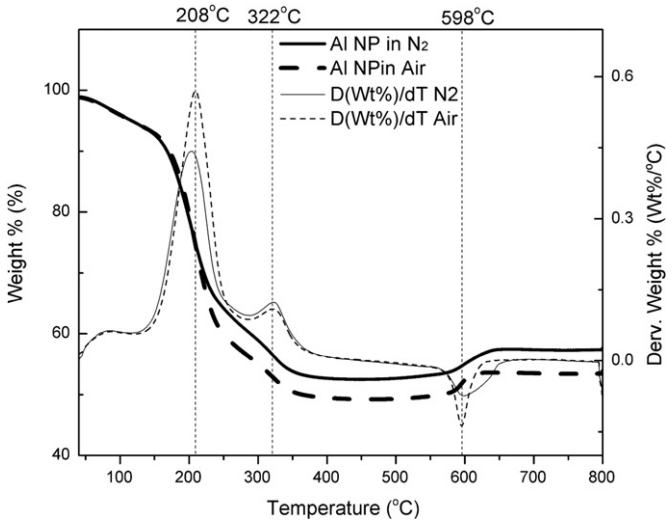

Fig. 2. Thermogravimetric analysis of aluminum nanoparticles (Al NPs) in the inert N_2 and air ambient for the temperature range between 40 and 800 °C.

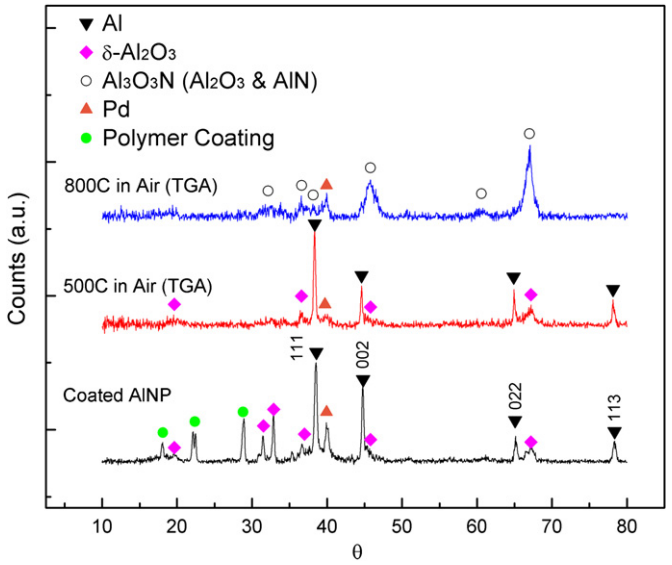

Fig. 3. X-ray diffraction patterns of coated aluminum nanoparticles (Al NP) and sintered ones in TGA at 500 and 800 °C in air ambient.

Notably, there is a reaction induced mass gain at 598 °C, which is 5% of the coated Al NP mass. The possible reactions that may lead to these mass changes were further studied using X-ray diffraction (XRD).

Fig. 3 shows the XRD patterns of the original Al NPs and sintered Al NPs, which were treated in TGA with air from room temperature to 500 °C and from room temperature to 800 °C, respectively. As expected and in agreement with the EDX characterization, the XRD pattern from the coated Al NPs exhibits peaks of aluminum, as well as peaks of delta phase Al_2O_3, coating material and the Pd (catalyst used for nitrocellulose coating). The aluminum structures in the coated Al NPs were characterized as (1 1 1) and (0 0 2) with minor peaks in the (0 2 2) and (1 1 3) planes. The Al_2O_3 peaks can find their source from the 1–2 nm interfacial layer between the coating nitrocellulose layer and the Al core. For the coated Al NPs, the three peaks near 17–28° belong to the coating nitrocellulose. For the 500 °C TGA sample, the aluminum components in the coated Al NP still exist. The coating material peaks, however, disappeared after 500 °C sintering. This results from the mass loss in the TGA data (shown in Fig. 2) and desorption of the coating shell. For the 800 °C TGA sample, the aluminum components in the coated Al NP disappeared and the broad peaks of Al_2O_3 and AlN are present. This XRD result relates to the mass gain in TGA near 600 °C, as shown in Fig. 2. Both TGA and XRD measurements suggest the following reactions between the aluminum in the core of the Al NPs and O_2/N_2 in air when the temperature is near 600 °C.

$$2Al + N_2 \rightarrow 2AlN \quad (3)$$

$$4Al + 3O_2 \rightarrow 2Al_2O_3 \quad (4)$$

$$6Al + 3O_2 + N_2 \rightarrow 2Al_3O_3N \quad (5)$$

The similar reactions have been observed by others when the aluminum micron particles were burned in air [15]. The composition was identified and is shown in Fig. 3. The reaction temperature between Al NPs and O_2/N_2 at 598 °C agrees with the data published by Trunnov et al. [16], which shows that 25–200 nm thick pure Al flakes have an oxidation temperature close to 600 °C. This comparison in the reaction temperature for coated Al NPs in this study and other aluminum particles in literature, on the other hand, shows that the protective coating does not remarkably interfere with the reactivity of the Al NP, which is important for processing the nano-thermite.

3.2. Nano-thermite reaction study

In order to study the reaction characteristics between passivated Al NPs and CuO NPs, such as the ignition temperature, the temperature corresponding to phase changes and reaction enthalpy, the DSC, and TGA data were obtained from the DTA measurement and processed. As mentioned previously, for the DTA measurements, the nano-thermite with the mass ratio of 3:1 (aluminum over CuO) was pressed into a pellet and then heated to 650 and 1100 °C in an inert Ar ambient. The effect from O_2 in air was excluded in the chamber. As shown in Fig. 4(a), the DSC curve shows a minor endothermic phase from 60 to 100 °C, which most likely comes from the phase change of the nitrocellulose coating. This point is followed by a highly exothermic peak starting at 200 °C and ending at 250 °C with a peak at 232 °C. In agreement with the TGA measurement, which shows a mass loss in the same temperature range, this exothermic temperature region results from the decomposition and subsequent desorption of the nitrocellulose shell. Another smaller exothermic peak at 304 °C was suspected from the similar process.

The next peak on the DSC curve occurs at 570 °C. This exothermic peak belongs to the thermite reaction, rather than the single melting process of solid aluminum. In order to investigate this peak, a XRD measurement was arranged on the sample that was sintered up to 650 °C in the Ar ambient. Fig. 4(b) shows the obtained XRD patterns that show a significant formation of Cu_2O and δ-Al_2O_3 together with some level of CuO. Based on this observation, first of all, one can exclude the contribution of the single melting process to this exothermic peak. It is possible, however, that a combined melting/reaction process exists for this temperature range. From the data provided by Levitas et al. [17], the melting point of 80 nm Al NP can be expected around 657 °C. Secondly, contrary to the reaction path described by Reaction (1), the following reaction is proposed for producing the products at about 570 °C:

$$Al + 3CuO \rightarrow 1/2\ Al_2O_3 + 3/2 Cu_2O \quad (6)$$

This agrees with the reaction kinetics reported by Umbrajkar et al. [18] where a micron-scale Al–CuO system was studied. In this study, Reaction (6) was validated for nano-scale Al–CuO systems. Fig. 4 shows no DSC peaks observed in the temperature

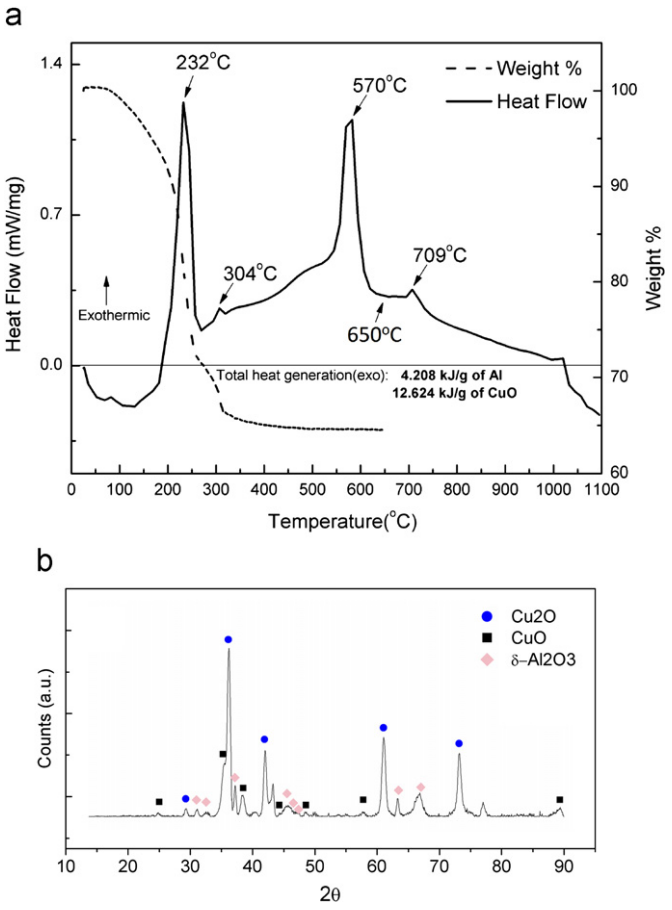

Fig. 4. (a) Comparison between the DSC curve (heat flow) taken from 0 to 1100 °C and the TGA curve (weight%) taken from 25 to 650 °C for 3:1 Al/CuO pellets. Heating rate: 5 °C/min. (b) XRD pattern taken from the sample that was sintered up to 650 °C.

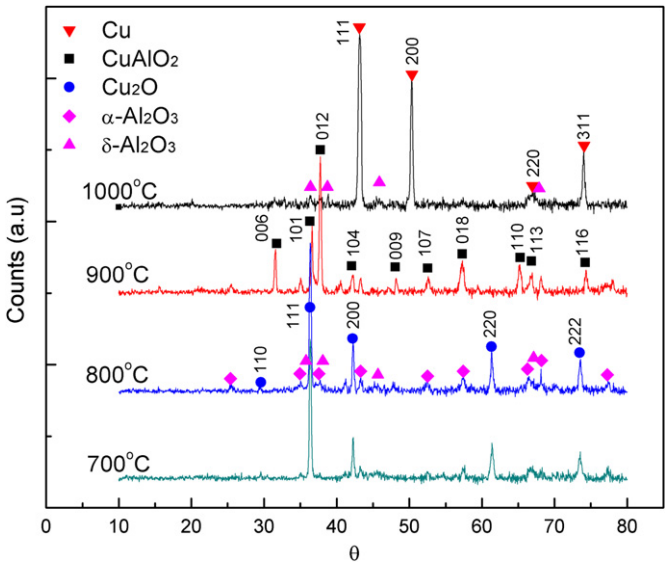

Fig. 5. X-ray diffraction patterns for sintered nano-thermites with a 3:1 (Al to CuO by mass) ratio. The samples were heated in vacuum furnace at 10^{-3} mbar and up to temperatures of 700, 800, 900, and 1000 °C, respectively.

Table 2
List of proposed reaction pathways for Al–CuO nano-thermite products observed at different temperatures. Q represents the energy release.

Conditions	Reactions	
At 570 °C	$Al+3CuO \rightarrow 1/2Al_2O_3+3/2Cu_2O+Q$	(6)
800–900 °C	$Al_2O_3+Cu_2O+Q \rightarrow 2CuAlO_2$	(7)
900–1000 °C	$CuAlO_2+Q \rightarrow 1/2Al_2O_3+Cu+O_2$	(8)

range between 570 and 709 °C. It is worthwhile to mention that Reaction (6) is a redox reaction that oxidizes Al to a +3 oxidation state and reduces Cu from +2 to +1 oxidation state. This reaction is responsible for the low-ignition-temperature thermite reaction made possible by nano-scale reactants.

The curious peak at 709 °C and the endothermic phase change near 1000 °C prompted an investigation on possible subsequent reactions and phase change processes above 570 °C. Comparing Fig. 4(b) with the XRD measurements on the product of nano-thermite reaction for higher temperatures (e.g., 700 and 800 °C as shown in Fig. 5), an increased intensity of α-Al_2O_3 is observed for samples sintered at and above 700 °C. This indicates that the 709 °C peak in Fig. 4 is associated with an exothermic phase change due to the further synthesis and progressive crystallization of α-Al_2O_3. It is interesting to observe in Fig. 5 that, a series of composition change processes occurred in the 800–1000 °C region. It starts with a mixture of Cu_2O and α-Al_2O_3 at 800 °C, converts into a mixture of $CuAlO_2$ and α-Al_2O_3 at 900 °C, and eventually ends with a mixture of pure Cu and δ-Al_2O_3. From the composition analysis and weight change processes observed above from each temperature, the reaction pathways for the Al–CuO nano-thermite with increasing temperatures are proposed and summarized in Table 2.

Note that from the above table, only Reaction (6) is exothermic. This means after the ignition at 570 °C, the energy release from Reaction (6) will sustain the phase changes described by Reactions (7) and (8). The formation of $CuAlO_2$ through Reaction (7) agrees with the previously reported study on the formation and decomposition kinetics of $CuAlO_2$ by Jacob and Alcock [19]. Reactions (7) and (8) are not thermodynamically favorable at lower temperatures and correlate well to the two DSC heat flow peaks at 710 and 1015 °C, as shown in Fig. 4. In order to investigate the effect of the fuel/oxidizer equivalence ratio on the reaction products, the XRD composition results for vacuum heating tests at 1000 °C are shown in Fig. 6 for mixtures with different Al/CuO mass ratios. The corresponding mass and mole ratios are consistent with the data shown in Table 1, and the discussion will be in terms of the mass ratio. In the fuel lean nano-thermite, such as the 1:1 Al/CuO mass ratio, the products of Cu_2O and $CuAlO_2$ were observed. In the slightly fuel rich mixture, such as the 2:1 Al/CuO mass ratio, the products of Cu_2O, $CuAlO_2$, and Cu were observed. In the fuel rich mixture, such as the 3:1 Al/CuO mass ratio, the product was mainly pure Cu. The signals from δ-Al_2O_3 were observed in all three XRD spectra. Although the current data were not collected for the purpose of a phase identification at a certain temperature, the reaction products agree reasonably with the phase diagram reported in Refs. [20,21]. As more aluminum component in the coated Al NPs were added into the system, the product of the thermite reaction at 1000 °C shifts from the mixture of $CuAlO_2$ and Cu_2O to mainly pure Cu. This phenomenon confirms with the reaction pathways proposed in Table 2. As noted from the previous section, the $CuAlO_2$ and Cu formation reactions, as shown in Reactions (7) and (8), are not thermodynamically favorable at lower temperatures, and Reaction (6) is the energy devoting step that allows for the occurrence of subsequent reactions. From the above discussions it is safe to deduce that in order to optimize the nano-thermites for achieving effective microjoining for microelectronics, the fuel/oxidizer ratio and temperature should be accurately controlled in order to trigger Reaction (6). In addition, the amount of nitrocellulose coating should

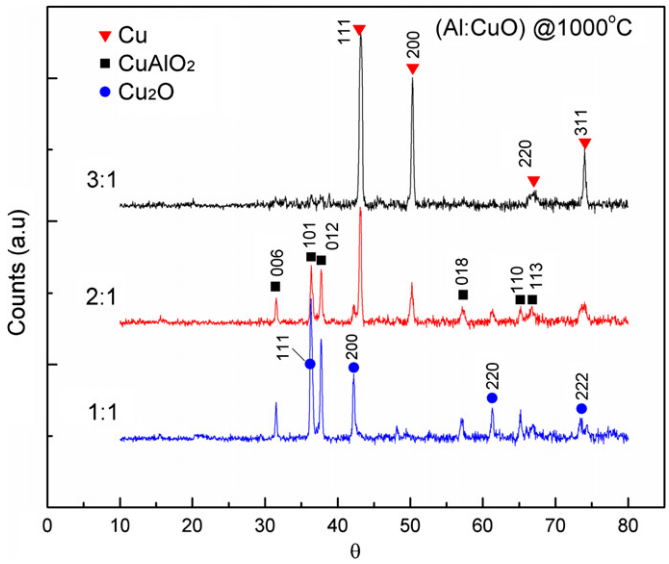

Fig. 6. X-ray diffraction patterns of nano-thermite of 3 to 1, 2 to 1, and 1 to 1, Al to CuO mass ratio that has been heated in vacuum furnace at 10^{-3} mbar and temperatures of 1000 °C.

be minimized since less aluminum component exists for the Al NPs with a thicker shell.

4. Conclusions

This study demonstrated a number of promising characteristics of Al NPs passivated with nitrocellulose. The experimental results showed that the passivation method for Al NPs was effective in stabilizing and protecting the Al NPs from a progressive oxidation in air. More importantly, the coating shell does not decrease the reactivity of the Al NP. Future studies may include the investigation on whether the coating shell would enhance the thermite reaction under adiabatic conditions. Through studying the reactive properties of Al NPs and CuO NPs, a low temperature solid-state reaction at 570 °C was observed for triggering the nano-thermite reaction. It corresponds to a significant decreased ignition temperature compared with the bulk aluminum. This decrease in the ignition temperature facilitates the Cu–Cu microjoining using nano-thermites. Furthermore, it was revealed that the nano-thermite reaction has a different reaction path (as shown in Reactions (6)–(8)) than the bulk thermite reaction. This provides guidance for future nano-thermite studies. More specifically, the composition after each step of the nano-thermite reaction pathways will be critical for the mechanical property analysis when the nano-thermite is used in welding and microjoining applications on different substrates.

Acknowledgements

This project is supported by NSERC (Natural Sciences and Engineering Research Council of Canada) through an Engage grant.

References

[1] D.R. Lide, CRC Handbook of Chemistry and Physics, CRC Press, Boca Raton, FL, 2005.
[2] K.L. Zhang, C. Rossi, M. Petrantoni, N. Mauran, J. Microelectromech. Syst. 17 (2008) 832–836.
[3] J.L. Cheng, H.H. Hng, H.Y. Ng, P.C. Soon, Y.W. Lee, J. Phys. Chem. Solids 71 (2010) 90–94.
[4] J. Sun, S.L. Simon, Thermochim. Acta 463 (2007) 32–40.
[5] C. Rossi, K. Zhang, D. Esteve, P. Alphonse, P. Tailhades, C. Vahlas, J. Microelectromech. Syst. 16 (2007) 919–931.
[6] S. Valliappan, J. Swiatkiewicz, J.A. Puszynski, Powder Technol. 156 (2005) 164–169.
[7] R. Shende, S. Subramanian, S. Hasan, S. Apperson, R. Thiruvengadathan, K. Gangopadhyay, S. Gangopadhyay, P. Redner, D. Kapoor, S. Nicolich, W. Balas, Propellants Explos. Pyrotech. 33 (2008) 122–130.
[8] K.J. Blobaum, M.E. Reiss, J.M.P. Lawrence, T.P. Weihs, J. Appl. Phys. 94 (2003) 2915–2922.
[9] S. Chowdhury, K. Sullivan, N. Piekiel, L. Zhou, M.R. Zachariah, J. Phys. Chem. C 114 (2010) 9191–9195.
[10] R.J. Jouet, A.D. Warren, D.M. Rosenberg, V.J. Bellitto, K. Park, M.R. Zachariah, Chem. Mater. 17 (2005) 2987–2996.
[11] K. Park, A. Rai, M.R. Zachariah, J. Nanopart. Res. 8 (2006) 455–464.
[12] T.J. Foley, C.E. Johnson, K.T. Higa, Chem. Mater. 17 (2005) 4086–4091.
[13] C. Dubois, P.G. Lafleur, C. Roy, P. Brousseau, R.A. Stowe, J. Propul. Power 23 (2007) 651–658.
[14] Y.S. Kwon, A.A. Gromov, J.I. Strokova, Appl. Surf. Sci. 253 (2007) 5558–5564.
[15] A. Gromov, A. Ilyin, A. Ditts, V. Vereshchagin, J. Eur. Ceram. Soc. 25 (2005) 1575–1579.
[16] M.A. Trunov, M. Schoenitz, X.Y. Zhu, E.L. Dreizin, Combust. Flame 140 (2005) 310–318.
[17] V.I. Levitas, M.L. Pantoya, G. Chauhan, I. Rivero, J. Phys. Chem. C 113 (2009) 14088–14096.
[18] S.M. Umbrajkar, M. Schoenitz, E.L. Dreizin, Thermochim. Acta 451 (2006) 34–43.
[19] K.T. Jacob, C.B. Alcock, J. Am. Ceram. Soc. 58 (1975) 192–195.
[20] S. Yi, K.P. Trumble, D.R. Gaskell, Acta Mater. 47 (1999) 3221–3226.
[21] K.A. Rogers, K.P. Trumble, B.J. Dalgleish, I.E. Reimanis, J. Am. Ceram. Soc. 77 (1994) 2036–2042.